

Article

Not peer-reviewed version

Hydrothermally Doping Valve Metal Nb into Titanate Nanofibers Structure for Potentially Engineering Bone Tissue

[Yang Tian](#) , Parker Cole , [Yiting Xiao](#) , Abdussamad Akhter , Trenton Collins , Lu Zhang , [Yan Huang](#) , [Ryan Tian](#) *

Posted Date: 5 April 2024

doi: 10.20944/preprints202404.0424.v1

Keywords: Nanosynthesis; Titanate nanofiber; Bone tissue engineering; Bone scaffold; Niobium dopant; Pro-bone elements



Preprints.org is a free multidiscipline platform providing preprint service that is dedicated to making early versions of research outputs permanently available and citable. Preprints posted at Preprints.org appear in Web of Science, Crossref, Google Scholar, Scilit, Europe PMC.

Copyright: This is an open access article distributed under the Creative Commons Attribution License which permits unrestricted use, distribution, and reproduction in any medium, provided the original work is properly cited.

Article

Hydrothermally Doping Valve Metal Nb into Titanate Nanofibers Structure for Potentially Engineering Bone Tissue

Yang Tian ^{1,2,†}, Parker Cole ^{3,†}, Yiting Xiao ^{4,†}, Abdussamad Akhter ⁵, Trenton Collins ⁵, Lu Zhang ⁶, Yan Huang ^{6,7} and Z. Ryan Tian ^{1,2,5,6,*}

¹ Material Science/Engineering, University of Arkansas, Fayetteville, AR 72701, USA.

² Institute for Nanoscience/Engineering, University of Arkansas, Fayetteville, AR 72701, USA.

³ Biomedical Engineering, University of Arkansas, Fayetteville, AR 72701, USA.

⁴ Biological and Agricultural Engineering, University of Arkansas, Fayetteville, AR 72701, USA.

⁵ Chemistry and Biochemistry, University of Arkansas, Fayetteville, AR 72701, USA.

⁶ Cell/Molecular Biology, University of Arkansas, Fayetteville, AR 72701, USA.

⁷ Animal Science, University of Arkansas, Fayetteville, AR 72701, USA.

* Correspondence: rtian@uark.edu

† The authors contribute to this work equally.

Abstract: Recent research efforts in bone tissue engineering have been primarily directed towards manufacture-viable synthesis of biomaterials that can significantly enhance the biocompatibilities and osteogenic capabilities on the new biomaterials. This paper presents a straightforward, cost-effective, optimized, and well-controlled hydrothermal synthesis of Nb-doped potassium titanate nanofibers in high-purity. Characterization data revealed that the Nb-doping potassium titanate maintained the crystal structure, showing great promise for applications in bone tissue engineering.

Keywords: nanosynthesis; titanate nanofiber; bone tissue engineering; bone scaffold; niobium dopant; pro-bone elements

1. Introduction

Nanomaterials possess the capability to bolster mechanical properties, release therapeutic ions or molecules into the adjacent environment to boost osteoblast cell recruitment, adhesion, growth, and differentiation; improve surface energy and protein adsorption, affect integrin binding; and function as a radiopacifier for improved visualization in X-ray imaging.[1–6] With the advent of nanotechnology, tissue engineering has advanced significantly, encompassing improvements ranging from architectural design and stability to multifunctional materials.

Given that bone is inherently a bio-nanocomposite, our objective has been to develop nanoscale substitutes of natural bone by utilizing novel materials that could promote bone tissue growth for bone regeneration. Recent studies have provided new insights into the mechanisms underlying the crucial role of nanotechnologies in orthopedic applications. Nanoscale characteristics such as grain size, pore dimensions and configuration, surface texture, surface-to-volume ratio, surface hydrophilicity, and related energetics are recognized as key contributors to such enhanced performance in bone tissue regeneration and integration[7]. To this end, a continuously expanding range of nanomaterials and nanotechnologies has been developed, examined, and applied within the field of bone tissue engineering[8–10].

Titanium dioxide has attracted growing interest with the merging of orthopedics and nanomaterial science. This is largely attributed to the well-established fact that Ti metal surfaces oxidize when in contact with air, forming a dense layer of native titanium dioxide (TiO₂) on the surface. Studies have revealed that anodization, a process to uniformly create an oxide surface coating, fosters the formation of a surface layer that is biologically compatible and promotes

osteogenesis. Advancements facilitated by nanomaterial chemistry have significantly advanced this field of study, with numerous laboratories achieving structural control over the TiO₂ layer in morphologies like nanofibers and nanotubes.[11,12] Remarkably, it has also been found that certain synthetic methods can lead to the formation of an ionic intermediate titanate structure. This layered clay-like crystalline structure, made up of edge-sharing TiO₆ octahedra intercalated with cations, has been recognized for its ability to facilitate hydroxyapatite formation in simulated body fluid (SBF)[13]. In a hydrothermal environment with an aqueous sodium (or potassium) hydroxide solution, powdery TiO₂ minerals, such as rutile and anatase, were involved in the chemical reaction to form either Na- or K-titanate nanotubes or nanowires, with the specific morphology significantly affected by the thermal conditions of the reaction. Thus-formed ionic layered structure acts as a cation "reservoir", allowing for potential ion exchange with cations in body fluids. This enables an autonomous, real-time balancing of cations in situ, aiding in the growth of bone tissue. Na/K-titanate is in a hypotonic state compared to the concentration of calcium (Ca²⁺) in the SBF inducing the ion exchange of Na⁺ or K⁺ ions with Ca²⁺. Subsequently, phosphate anions in the body fluid, including (PO₃)³⁻, (HPO₃)²⁻, and (H₂PO₃)⁻, interact with the Ca²⁺ on the titanate surface. This interaction leads to the formation of hydrated calcium phosphate, known as hydroxyapatite, a critical component of natural bone essential for creating an osteogenic/osteoconductive environment[13].

In addition, the nanomaterials with pro-bone elements like Zirconium (Zr), Niobium (Nb), or Tantalum (Ta) have been demonstrated to enhance the performance of osteointegration[14–17]. However, the practical implementation of these pro-bone element oxides has been hindered by the often-elevated costs and synthesis complexities. Therefore, doping titanate nanofibers with pro-bone elements emerges as an advantageous alternative approach to create novel bone implant materials. In this work, we systematically conducted nanosynthesis to produce long and pristine Nb-doped titanate nanofibers with strong market feasibility for orthopedic implants. The optimization of doping was verified through the analysis of characterization data obtained from scanning electron microscopy with an energy-dispersive elemental analyzer (SEM-EDX) and X-ray diffraction (XRD).

2. Materials and Methods

2.1. Nanofiber Synthesis

The Nb-doped potassium titanate nanofibers were prepared following a published protocol[18–23] with some modifications. Briefly, in a Teflon cup containing 50mL water solution of 10M KOH, 500mg of TiO₂ powder (Aeroxide P25) was added to the Teflon and stirred for about 5 minutes with a Teflon-coated magnetic stirring bar on an electrical stirrer. Thereafter, Niobium oxide powder (chemical grade, from Alfa Aesar) was mixed with the KOH solution to form a mixture upon stirring. Here, the molar ratio of Nb-dopant to Titanate was widely varied from 1% - 4%.

Next, the mixture containing Teflon cup was sealed in an autoclave container, heated in an oven at 240 °C for 72 hours and then cooled down in air. The white powdery product was collected, water-washed until pH = 7, and finally air-dried for the characterizations. To keep the nanofiber lattice intact, it is important to do the water-washing step carefully, as detailed separately below.

2.2. Post Synthesis Washing

The fibers were formed as a slurry from the high alkalinity environment in the autoclave treatment. To remove the residual KOH, the white slurry went through a well-controlled neutralization process. The nanofiber slurry was first centrifuged for 5 min at 4000 rpm. The supernatant was decanted and then mixed with deionized water to form another slurry with a lower KOH content, which was repeated until the supernatant's pH=7.

2.3. Characterization

The SEM-EDX analysis was carried out on the FEI Nova NanoLab 200 to assess nanofiber morphology and chemical composition. Typically, the fiber sample was placed on an aluminum holder to let the sample dry in air. Once dried, the holder was placed in a plasma sputtering coater with an Au target to coat the sample surface with Au. The XRD was performed with the Rigaku MiniFlex II Desktop X-ray diffractometer using monochromatized Cu-K α ($\lambda = 1.5406 \text{ \AA}$) at 30 kV and 15 mA, in the range of 2θ from 5° to 60° at a speed of $1^\circ/\text{min}$. to assess crystal structure.

3. Results & Discussion

3.1. Niobium Doping

The Nb-doped potassium titanate nanofibers underwent self-assembly, forming a bone-mimetic bio-scaffold structure upon desiccation as illustrated in **Figure 1**. These self-assembled nanowires created porous structures, facilitating effective bone tissue adhesion to the bio-scaffold. Moreover, the increased surface area provided by these structures enhances osteoblast cell adhesion.

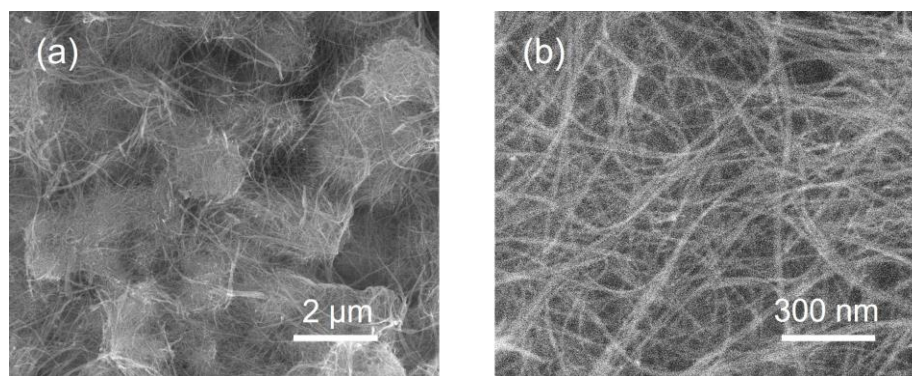


Figure 1. SEM Micrographs of Nb-Doped Potassium Titanate.

At higher magnification (**Figure 2(a)**), the clean and well-crystallized long nanofibers in self-entangled sheets can be clearly seen, which is a characteristic of the Nb-doped potassium titanate nanofibers. The nanofiber length extends into the microns range whereas the width of these fibers is under 100 nm. Additionally, **Figure 2(a)** shows the relatively smooth surface of the high length to width ratio (or aspect ratio) nanofibers, suggesting an optimal control over the nanosynthesis parameters to achieve the uniformly distributed Ta-doping throughout the lattice.

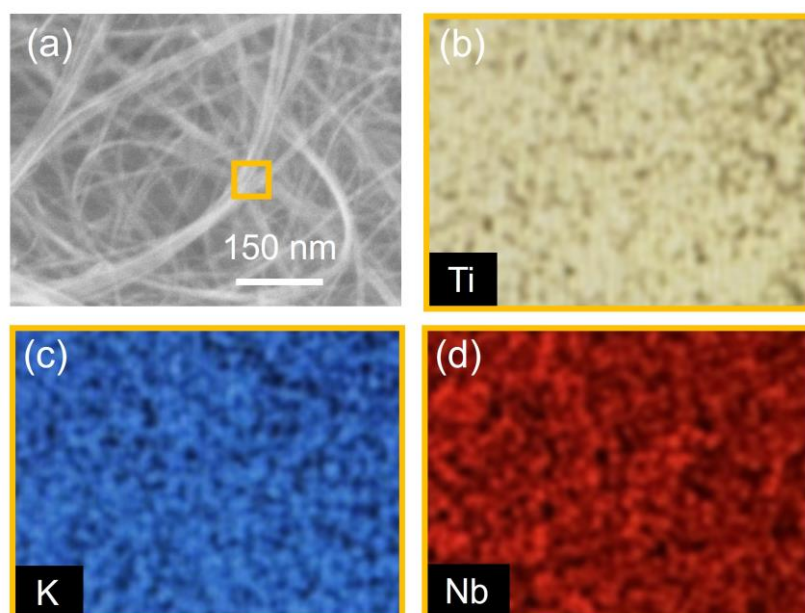


Figure 2. Element Dispersive EDX Mapping of the Nb-Doped Potassium Titanate Nanofibers. (a) The high-resolution SEM of Nb-doped potassium with the yellow box for EDX mapping. The EDX mapping showed (b) K, (c) Ti, and (d) Nb are evenly distributed on the titanate nanofibers.

On the EDX map, the Nb dopants (**Figure 2(d)**) are distributed on the fibers showing overlap with the Ti species (**Figure 2(b)**), indicating the lattice building blocks of the smaller $[\text{TiO}_6]$ octahedra more than the larger $[\text{NbO}_6]$ octahedra. Seemingly, the $[\text{NbO}_6]$ octahedra are well-dispersed allowing for the structural distortion of each $[\text{NbO}_6]$ octahedron to not destroy the lattice structural continuity. The high dispersion of Nb dopant in the nanofiber structure suggests the optimal doping conditions that support **Figure 1**.

The nanofiber crystal structure can be characterized using the XRD patterns (**Figure 3**). All the XRD peaks of (200), (110), (310), $(31\bar{2})$, $(40\bar{4})$, and (020) can be assigned to the layered $\text{K}_2\text{Ti}_6\text{O}_{13}$ titanate lattice (JCPDS No. 40-0403). No residual impurity was detected, as evidenced by no extra peaks in the XRD pattern due to the XRD detection limit, which indicates that the larger $[\text{NbO}_6]$ octahedron is well doped in the titanate crystal structure to maintain the lattice integrity and nanofiber structure.

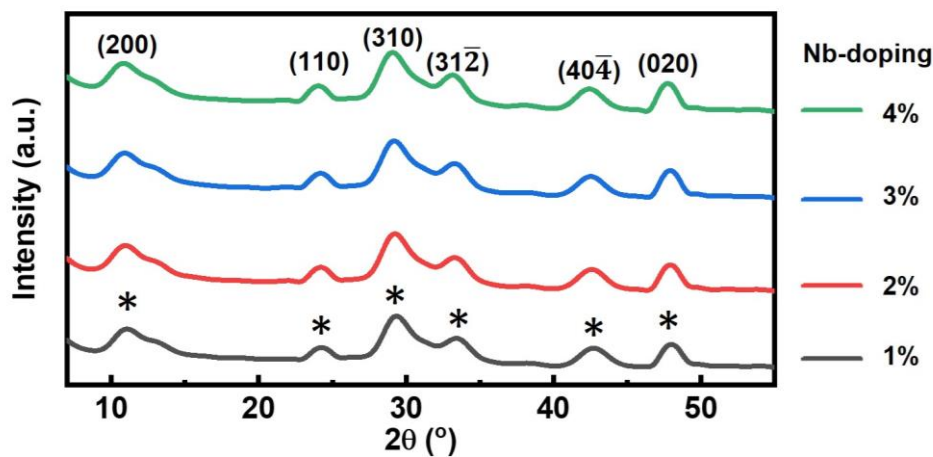


Figure 3. X-Ray Diffraction of Nb-Doped Potassium Titanate Nanofibers with variant doping percentage.

Comparing the XRD patterns with and without doping (**Figure 4(a)**), the large Nb-dopant increases the d-space between adjacent titanate sheets by shifting the XRD peak to $d_{(200)} = 8.18147 \text{ \AA}$ (or a lower 2-theta angle at $2\theta = 10.81^\circ$) [20,24]. This is in contrast with the undoped nanofiber's smaller d-space of $d_{(200)} = 7.7415 \text{ \AA}$ at a higher 2-theta angle ($2\theta = 11.43^\circ$). This interlayer spacing expansion is indicative of Nb substitutional doping within the titanate lattice. More specifically, the ionic radius of Nb^{5+} (64 pm) is larger than that of Ti^{4+} (53 pm) which leads to Nb^{5+} species replacing Ti^{4+} within the titanate lattice. Substitutional doping of larger ions within the native lattice increases lattice parameters and cell volume resulting in shifts to lower diffraction angles [25]. Moreover, the doped samples XRD patterns show no structural impurity. This is because all the XRD peaks are in the same width and can be indexed to that of potassium titanate, as others including those reported in literature by our lab [18–20].

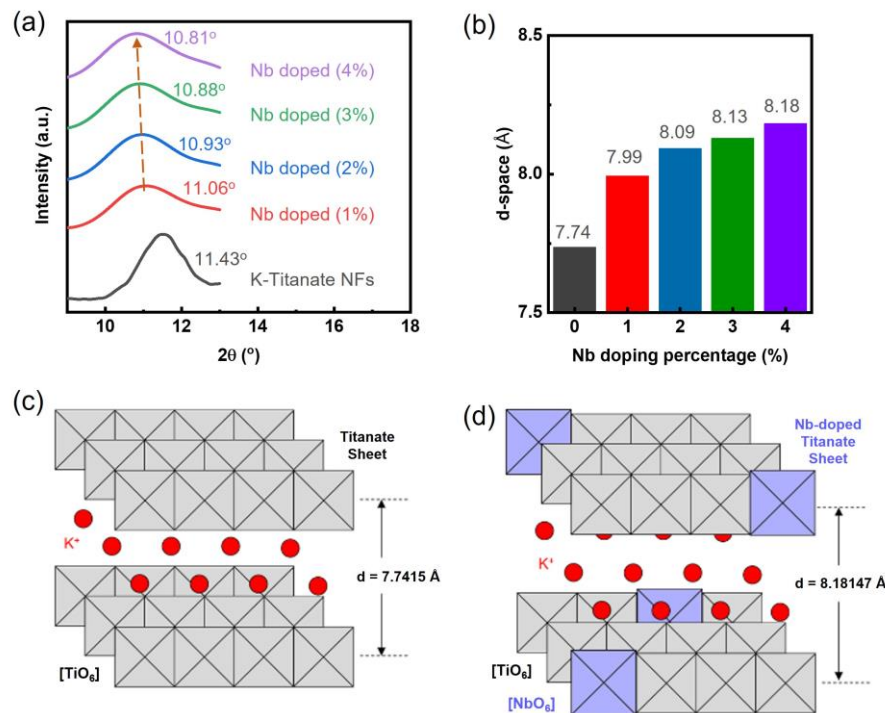


Figure 4. (a) XRD analysis of Nb-doped potassium titanate nanofibers with (b) d-space. (c) and (d) Nb-dopant impact on the titanate crystal structure.

Evidently, within the K-titanate nanofiber's clay-like layered crystal structure, the Ti^{4+} -based $[\text{TiO}_6]$ octahedra have undergone partial substitution by the Nb^{5+} -based $[\text{NbO}_6]$ octahedra, confirming the intentional doping of Nb^{5+} . From a steric perspective, the larger $[\text{NbO}_6]$ compared to $[\text{TiO}_6]$ would naturally position itself on the nanofiber surface to reduce perturbations in the predominantly $[\text{TiO}_6]$ crystal lattice. Such surface-exposed $[\text{NbO}_6]$ units have been recognized to facilitate bone-tissue adhesion, as corroborated by previous studies[1,14,26]. Additionally, the proximal interlayer K^+ cations to the $[\text{NbO}_6]$ in the K-titanate nanofiber are predisposed to be swiftly substituted by Ca^{2+} cations from body fluids. This accelerates the formation of hydrated calcium phosphates, or hydroxyapatite, on the nanofiber, consistent with findings from other research groups using SBF[13,27]. The robust interaction between the hydroxyapatite layer and the underlying titanate nanofiber ensures sustained bone tissue adhesion on the hydroxyapatite-supported nanofiber, crafting an optimal osteogenic/osteoconductive milieu[13]. Therefore, the refined surface characteristics of titanate nanofibers present a complementary approach to existing methodologies, enhancing the osteoconductivity of bone-scaffolds[14,26,28]. Fundamentally, this research introduces a pioneering and economically viable technique for incorporating Nb (V) into the titanate nanofiber matrix, marking a significant stride in the realm of orthopedic nanomedicine.

5. Conclusions

Niobium-doped potassium titanate nanofibers have been successfully produced using a simple hydrothermal method. This approach is notably innovative, particularly in the field of orthopedic nanomedicine, as far as we are aware. After doping, the nanofibers maintained their morphology, chemical composition, and crystallinity, suggesting that the hydrothermal method used for doping the crystal framework is effective. Moreover, the dopant concentrations were carefully controlled to ensure no negative impact on the nanofiber's lattice structure. This is crucial for preserving their desired properties for the intended uses. To evaluate the impact of this material in the field of bone tissue engineering, nanofibers with different concentrations of Nb dopant have been studied in vitro to determine their biocompatibility and osteogenic capabilities.

The logical subsequent step, which involves examining these nanofibers with systematically varied concentrations of Nb dopant for their biocompatibility and osteogenic potential, is currently in progress. Evaluating the interaction of these doped nanofibers with bone cells will provide crucial information regarding their viability as candidates for bone implants. This assessment of biocompatibility plays a vital role in determining the suitability of materials for medical applications.

A forward-thinking approach to expand on this research involves doping the titanate nanofibers with, for instance, dual oxide dopants. This method could enable the investigation of a more diverse array of bone implants, offering extensive physiological adaptability. Comprehending the effects of doping biocompatible transition metals on the physical and chemical characteristics of the nanofiber-based bone implant is important for customizing the biomaterials according to each specific application.

Creating a broad and new family of doped titanate nanofibers, each with unique compositions and properties, represents an intelligent strategy for allowing researchers to investigate the effects of doping variations on the material's attributes and efficacy. Such data could be crucial in fine-tuning these materials for targeted applications in bone tissue engineering or other fields.

Author Contributions: Investigation, YT, YX, AA, and TC; writing—original draft preparation, YT, ZRT; writing—review and editing, YT, PC, LZ, YH, and ZRT. All authors have read and agreed to the published version of the manuscript.

Data Availability Statement: Applicable for reasonable request.

Funding: N/A.

Acknowledgments: The team would like to thank Paula Prescott and Connie Dixon for ordering lab supplies and managing financial reimbursement. The team also would like to thank Kz Shein, Zay Lynn, and David N. Parette for the technical support.

Conflicts of Interest: The authors declare no conflict of interest. The funders had no role in the design of the study; in the collection, analyses, or interpretation of data; in the writing of the manuscript, or in the decision to publish the results.

References

1. Zhang, B.; Li, J.; He, L.; Huang, H.; Weng, J. Bio-Surface Coated Titanium Scaffolds with Cancellous Bone-like Biomimetic Structure for Enhanced Bone Tissue Regeneration. *Acta Biomaterialia* **2020**, *114*, 431–448. <https://doi.org/10.1016/j.actbio.2020.07.024>.
2. Min, Q.; Liu, J.; Zhang, Y.; Yang, B.; Wan, Y.; Wu, J. Dual Network Hydrogels Incorporated with Bone Morphogenic Protein-7-Loaded Hyaluronic Acid Complex Nanoparticles for Inducing Chondrogenic Differentiation of Synovium-Derived Mesenchymal Stem Cells. *Pharmaceutics* **2020**, *12* (7), 613. <https://doi.org/10.3390/pharmaceutics12070613>.
3. Wu, T.; Li, B.; Wang, W.; Chen, L.; Li, Z.; Wang, M.; Zha, Z.; Lin, Z.; Xia, H.; Zhang, T. Strontium-Substituted Hydroxyapatite Grown on Graphene Oxide Nanosheet-Reinforced Chitosan Scaffold to Promote Bone Regeneration. *Biomaterials Science* **2020**, *8* (16), 4603–4615. <https://doi.org/10.1039/D0BM00523A>.
4. Oudadesse, H.; Najem, S.; Mosbahi, S.; Rocton, N.; Refifi, J.; El Feki, H.; Lefeuvre, B. Development of Hybrid Scaffold: Bioactive Glass Nanoparticles/Chitosan for Tissue Engineering Applications. *Journal of Biomedical Materials Research Part A* **2021**, *109* (5), 590–599. <https://doi.org/10.1002/jbm.a.37043>.
5. Nie, L.; Deng, Y.; Li, P.; Hou, R.; Shavandi, A.; Yang, S. Hydroxyethyl Chitosan-Reinforced Polyvinyl Alcohol/Biphasic Calcium Phosphate Hydrogels for Bone Regeneration. *ACS Omega* **2020**, *5* (19), 10948–10957. <https://doi.org/10.1021/acsomega.0c00727>.
6. Maji, K.; Dasgupta, S.; Bhaskar, R.; Gupta, M. Photo-Crosslinked Alginate Nano-Hydroxyapatite Paste for Bone Tissue Engineering. *Biomedical Materials* **2020**, *15* (5). <https://doi.org/10.1088/1748-605X/ab9551>.
7. Gao, C.; Wei, D.; Yang, H.; Chen, T.; Yang, L. Nanotechnology for Treating Osteoporotic Vertebral Fractures. *International Journal of Nanomedicine* **2015**, *10*, 5139–5157. <https://doi.org/10.2147/IJN.S85037>.
8. Venkataramana, C.; Botsa, S. M.; Shyamala, P.; Muralikrishna, R. Photocatalytic Degradation of Polyethylene Plastics by NiAl₂O₄ Spinel-Synthesis and Characterization. *Chemosphere* **2021**, *265*, 129021. <https://doi.org/10.1016/j.chemosphere.2020.129021>.

9. Saravanan, S.; Vimalraj, S.; Anuradha, D. Chitosan Based Thermoresponsive Hydrogel Containing Graphene Oxide for Bone Tissue Repair. *Biomedicine & Pharmacotherapy* **2018**, *107*, 908–917. <https://doi.org/10.1016/j.biopha.2018.08.072>.
10. Mohammadi, M.; Mousavi Shaegh, S. A.; Alibolandi, M.; Ebrahimzadeh, M. H.; Tamayol, A.; Jaafari, M. R.; Ramezani, M. Micro and Nanotechnologies for Bone Regeneration: Recent Advances and Emerging Designs. *Journal of Controlled Release* **2018**, *274*, 35–55. <https://doi.org/10.1016/j.jconrel.2018.01.032>.
11. Aldaadaa, A.; Qaysi, M.; Knowles, J. Physical Properties and Biocompatibility Effects of Doping SiO₂ and TiO₂ into Phosphate-Based Glass for Bone Tissue Engineering. *Journal of Biomaterials Applications* **2018**, *33* (2), 271–280. <https://doi.org/10.1177/08853282187888>.
12. Hashemi, A.; Ezati, M.; Mohammadnejad, J.; Houshmand, B.; Faghihi, S. Chitosan Coating of TiO₂ Nanotube Arrays for Improved Metformin Release and Osteoblast Differentiation. *International Journal of Nanomedicine* **2020**, *15*, 4471–4481. <https://doi.org/10.2147/IJN.S248927>.
13. Liang, F.; Zhou, L.; Wang, K. Apatite Formation on Porous Titanium by Alkali and Heat-Treatment. *Surface and Coatings Technology* **2003**, *165* (2), 133–139. [https://doi.org/10.1016/S0257-8972\(02\)00735-1](https://doi.org/10.1016/S0257-8972(02)00735-1).
14. Marins, N. H.; Lee, B. E. J.; e Silva, R. M.; Raghavan, A.; Villarreal Carreño, N. L.; Grandfield, K. Niobium Pentoxide and Hydroxyapatite Particle Loaded Electrospun Polycaprolactone/Gelatin Membranes for Bone Tissue Engineering. *Colloids and Surfaces B: Biointerfaces* **2019**, *182*, 110386. <https://doi.org/10.1016/j.colsurfb.2019.110386>.
15. Cadafalch Gazquez, G.; Chen, H.; Veldhuis, S. A.; Solmaz, A.; Mota, C.; Boukamp, B. A.; van Blitterswijk, C. A.; ten Elshof, J. E.; Moroni, L. Flexible Yttrium-Stabilized Zirconia Nanofibers Offer Bioactive Cues for Osteogenic Differentiation of Human Mesenchymal Stromal Cells. *ACS Nano* **2016**, *10* (6), 5789–5799. <https://doi.org/10.1021/acsnano.5b08005>.
16. Hwang, C.; Park, S.; Kang, I.-G.; Kim, H.-E.; Han, C.-M. Tantalum-Coated Polylactic Acid Fibrous Membranes for Guided Bone Regeneration. *Materials Science and Engineering: C* **2020**, *115*, 111112. <https://doi.org/10.1016/j.msec.2020.111112>.
17. Zhang, J.; Huang, D.; Liu, S.; Dong, X.; Li, Y.; Zhang, H.; Yang, Z.; Su, Q.; Huang, W.; Zheng, W.; Zhou, W. Zirconia Toughened Hydroxyapatite Biocomposite Formed by a DLP 3D Printing Process for Potential Bone Tissue Engineering. *Materials Science and Engineering: C* **2019**, *105*, 110054. <https://doi.org/10.1016/j.msec.2019.110054>.
18. Dong, W.; Cogbill, A.; Zhang, T.; Ghosh, S.; Tian, Z. R. Multifunctional, Catalytic Nanowire Membranes and the Membrane-Based 3D Devices. *J. Phys. Chem. B* **2006**, *110* (34), 16819–16822. <https://doi.org/10.1021/jp0637633>.
19. Dong, W.; Zhang, T.; Epstein, J.; Cooney, L.; Wang, H.; Li, Y.; Jiang, Y.-B.; Cogbill, A.; Varadan, V.; Tian, Z. R. Multifunctional Nanowire Bioscaffolds on Titanium. *Chem. Mater.* **2007**, *19* (18), 4454–4459. <https://doi.org/10.1021/cm070845a>.
20. Cole, P.; Tian, Y.; Thornburgh, S.; Malloy, M.; Roeder, L.; Maulding, M.; Huang, Y.; Tian, Z. R. Hydrothermal Synthesis of Valve Metal Zr-Doped Titanate Nanofibers for Bone Tissue Engineering. *Nano and Medical Materials* **2023**, *3* (2), 249. <https://doi.org/10.59400/nmm.v3i2.249>.
21. Xiao, Y.; Tian, Y.; Zhan, Y.; Zhu, J. Degradation of Organic Pollutants in Flocculated Liquid Digestate Using Photocatalytic Titanate Nanofibers: Mechanism and Response Surface Optimization. *Front. Agr. Sci. Eng.* **2023**, *10* (3), 492–502. <https://doi.org/10.15302/J-FASE-2023503>.
22. Ye, X.; Tian, Y.; Gao, M.; Cheng, F.; Lan, J.; Chen, H.; Lanoue, M.; Huang, S.; Tian, Z. R. Efficient Photocatalytic Core-Shell Synthesis of Titanate Nanowire/rGO. *Catalysts* **2024**, *14* (4), 218. <https://doi.org/10.3390/catal14040218>.
23. Tian, Y.; Zhang, L.; Xiao, Y.; Collins, T.; Akhter, A.; Huang, Y.; Tian, Z. R. Mo-Doped Titanate Nanofibers from Hydrothermal Syntheses for Improving Bone Scaffold. *Characterization and Application of Nanomaterials* **2024**, *7* (1), 3587. <https://doi.org/10.24294/can.v7i1.3587>.
24. Yuan, Z.-Y.; Zhang, X.-B.; Su, B.-L. Moderate Hydrothermal Synthesis of Potassium Titanate Nanowires. *Appl. Phys. A* **2004**, *78* (7), 1063–1066. <https://doi.org/10.1007/s00339-003-2165-x>.
25. Bi, H.; Zhu, S.; Liang, Y.; Jiang, H.; Li, Z.; Wu, S.; Wei, H.; Chang, C.; Wang, H.; Cui, Z. Nb-Doped TiO₂ with Outstanding Na/Mg-Ion Battery Performance. *ACS Omega* **2023**, *8* (6), 5893–5900. <https://doi.org/10.1021/acsomega.2c07689>.
26. Balbinot, G. de S.; Bahlis, E. A. da C.; Visioli, F.; Leitune, V. C. B.; Soares, R. M. D.; Collares, F. M. Polybutylene-Adipate-Terephthalate and Niobium-Containing Bioactive Glasses Composites: Development of Barrier Membranes with Adjusted Properties for Guided Bone Regeneration. *Materials Science and Engineering: C* **2021**, *125*, 112115. <https://doi.org/10.1016/j.msec.2021.112115>.
27. Wang, X.; Liu, S. J.; Qi, Y. M.; Zhao, L. C.; Cui, C. X. Behavior of Potassium Titanate Whisker in Simulated Body Fluid. *Materials Letters* **2014**, *135*, 139–142. <https://doi.org/10.1016/j.matlet.2014.07.145>.
28. Capanema, N. S. V.; Mansur, A. A. P.; Carvalho, S. M.; Silva, A. R. P.; Ciminelli, V. S.; Mansur, H. S. Niobium-Doped Hydroxyapatite Bioceramics: Synthesis, Characterization and In Vitro Cytocompatibility. *Materials* **2015**, *8* (7), 4191–4209. <https://doi.org/10.3390/ma8074191>.

Disclaimer/Publisher's Note: The statements, opinions and data contained in all publications are solely those of the individual author(s) and contributor(s) and not of MDPI and/or the editor(s). MDPI and/or the editor(s) disclaim responsibility for any injury to people or property resulting from any ideas, methods, instructions or products referred to in the content.